FATIGUE AND FRACTURE BEHAVIOUR OF A LASER HEAT TREATED MARTENSITIC HIGH-NITROGEN TOOL STEEL

M.Heitkemper[1], C.Bohne[2], A.Pyzalla[2], A.Fischer[1]

[1]Werkstofftechnik, Universitaet Essen, 45117 Essen, Germany
[2]Hahn-Meitner Institut, Abt. Werkstoffe, 14109 Berlin, Germany

ABSTRACT

High nitrogen tool steels offer a superior corrosion resistance compared to conventional, Nitrogen-free tool steels at similar mechanical and tribological properties. For this reason they are nowadays applied for ball bearings in aircraft industry. A laser-surface treatment can lead to a further improvement of this combination of properties. The aim of a research project is to improve the tribological properties and at the same time keep up or enhance the corrosion resistance as well as the fatigue behaviour. The laser heat-treatment leads to a mixture of martensite and retained austenite. Thus, the martensitic regions show an increased hardness of about 700 HV10, while the austenitic regions are as soft as 400 HV10. To determine the influence of a laser-surface treatment on fatigue cyclic 4-point-bending tests in laboratory air as well an in artificial sea water (3%NaCl, 25°C) have been performed. The fatigue and fracture behaviour are mostly influenced by the refinement of the microstructure and the generation of compressive residual stresses. In addition the retained austenite and its stress induced transformation into martensite affects the fatigue behaviour. The residual stresses generated during heat treatment have a significant influence on crack initiation, while those generated during the transformation of the retained austenite have only a minor influence on crack propagation.

KEYWORDS

laser surface heat treatment, high-Nitrogen tool steel, fatigue, fracture mechanics, corrosion, residual stresses

INTRODUCTION

Martensitic high-Nitrogen steels (HNS) offer a favourable combination of tribological, chemical and mechanical properties. While the wear behaviour is comparable to conventional tool steels the corrosion resistance is significantly higher. For this reason they are already applied as materials for roller bearings of gas turbines and fuel pumps as well as for ball screws of thread gears in aerospace applications [1, 2, 3]. The good wear behaviour can be attributed to the fine dispersion of precipitates, which is governed by Nitrogen. The reason for the improved corrosion resistance is brought about by the high contents of Cr, Mo and N dissolved within the martensitic matrix. In many cases it is necessary to use cold-work tool steels in a tempered state in order to reduce the amount of retained austenite. In this heat treated condition Cr, Mo, and N are bound within precipitates. Within a DFG (German Research Council) funded research project the effect of a surface heat treatment by laser on microstructure and properties of HNS is investigated. During this kind of short time heat treatment nitrides are partly dissolved and new martensite is generated [4]. The dissolution of nitrides lays off some Cr and N and increases the resistance against pitting corrosion [5]. The

newly generated martensite brings about high compressive residual stresses and a higher surface hardness and distinctly improves the wear resistance under sliding wear in air as well as in artificial sea water [6]. Both should improve the life time of wear and corrosion resistant parts and tools. But, the endurance life might be limited by deteriorated fatigue and fracture properties.

In this paper the influence of the laser surface heat treatment on the fatigue properties is presented and discussed. With respect to the application of the HNS X30CrMoN15 1 (1.4108 = AMS5898) in aerospace industries the tests have been carried out in air as well as in artificial sea water.
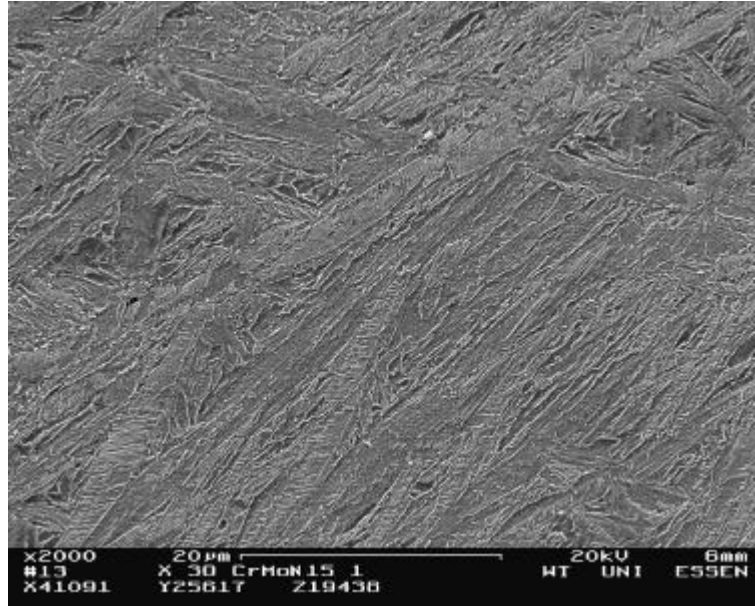

Figure 1: Tempered Martensite of Heat Treated X30CrMoN15 1 with less than 2 % Retained Austenite.

EXPERIMENTAL PROCEDURES

Materials and Heat Treatments
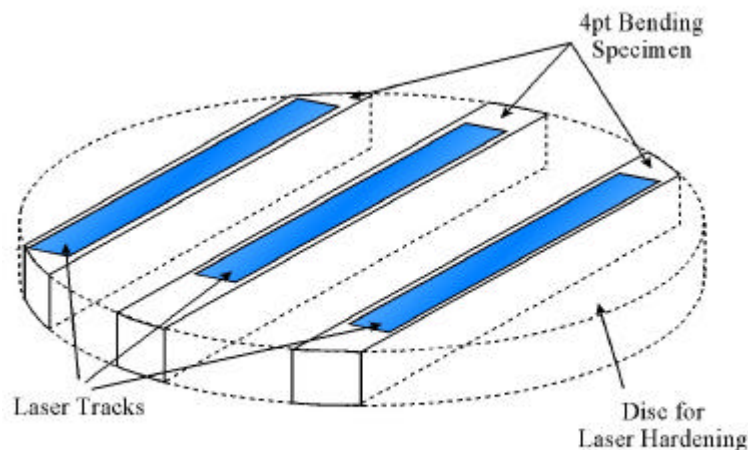Before the laser treatments HNS discs of 100 mm diameter and 10 mm thickness were heat treated as

Figure 2: Design of the Specimens for Laser Surface Heat Treatment and Fatigue Testing.

follows: 30min/1200°C/oil+10min/-196°C/air+3x2h/620°C/air. The chemical composition of the HNS is given in Table 1. Figure 1 shows the microstructure, which consists of tempered martensite with less than 2 vol.-% of retained austenite (RA). Afterwards the specimens were laser-heat treated using a 3kW Nd:YAG-laser. The power of the laser was controlled by the maximum surface temperature T_{max} in the heat treated area. The beam had a cross section of 14 x 1,8 mm transversally to the moving-direction (Figure 2) and was moved with a speed of 100 mm/min over the surface under an atmosphere of 15 l/min N_2 and 0,13

l/min O_2. After this heat treatment all specimens were scrutinised as to their microstructures, residual stresses, wear, and corrosion properties which in detail is reported elsewhere [4, 5].

Table 1: Chemical Composition of the Martensitic High-Nitrogen Steel X30CrMoN15 1, 1.4108 = AMS5898 according to the Steel Manufacturers Specification.

Fe	C	Si	Mn	Cr	Ni	Mo	N
bal.	0.25-0.35	< 1	< 1	14-16	< 0.5	0.85-1.1	0.3-0.5

Fatigue Testing and Fractography

The fatigue specimens were cut out of the lasered discs by mechanical wet cutting and afterwards machined and ground on all areas - except the laser hardened surfaces – (Figure 1). It has to be noticed that two types of specimens were provided. One group contains specimens of 12 mm width, which comprise the hardened zones, only. The second group of 16 mm width embody the tempered zones as well. These bars were loaded cyclically in a 4-point bending (4PB) test device (Figure 3), which was mounted within a servohydraulic test rig. The load range of the constant stress amplitude tests was chosen between 225 and 630 MPa at 20 Hz and an R-value of 0.1. In order to carry out tests in artificial sea water (3 % NaCl in aqua dest.) at room temperature the specimens were placed inside a rubber tube. This set up allows a continuous flow of the artificial sea water brought about by a small aquarium water pump. The water temperature was measured by a thermocouple and scattered between 20 and 30 °C. Under both conditions (dry/3%NaCl) the specimens were fatigued to fracture and the results were plotted in Wöhler-diagrams (S-N curves). Afterwards the fracture surfaces were investigated in making use of a scanning electron microscope.
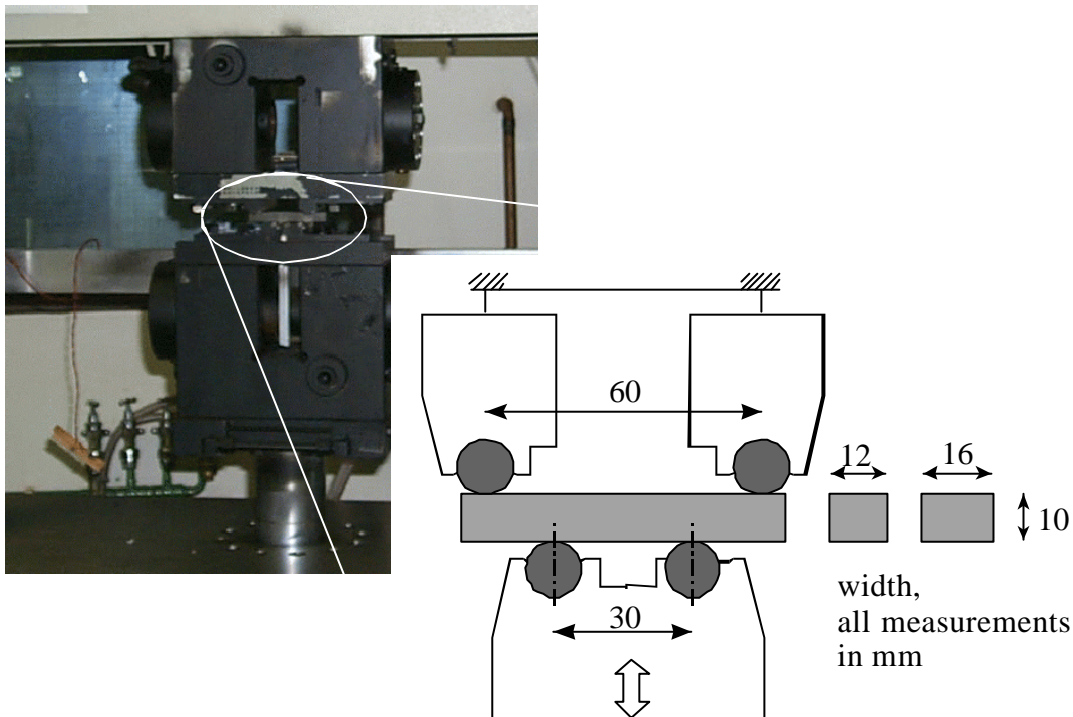

Figure 3: Test Rig for Cyclic 4-Point Bending in Air

RESULTS AND DISCUSSION

Microstructure and Residual Stresses

Figure 4 shows the results of the microstructural examinations after a series of laser heat treatments at different maximum temperatures [4, 5]. At about 950°C the surface hardness and the c_m/a_m-ratio, which represents the tetragonal distortion of the newly generated martensite, increase. The hardness reaches its maximum value slightly above 1000 °C as a result of the increasing distortion of the martensite. Above that temperature hardness decreases by the governing influence of the increasing amount of RA, which is markedly stabilised by N. According to the nature of the temperature field one has to distinguish between

two areas within a lasered track: The hardened zones in the middle of a track with compressive residual stresses and the softer tempered zones at the boundaries of the lasered tracks with tensile residual stresses.

In order to gain a high amount of RA directly at the surface, which has a beneficial influence on the chemical and tribological properties [4-6] T_{max} for the laser surface treatments of the specimens was chosen to 1100 °C. Thus, there is a gradient of RA, hardness and residual stresses with the distance from the surface. Due to the fact that there is 100 % RA at the surface, the maximum hardness value of 750 HV is at a depth of about 100 µm. The residual stresses alter from compression to tension at about 140 µm below the surfaces. One has to keep in mind that the beneficial effects of laser hardening might disappear at a distance of about 140 µm from the surface, if the laser heat treatment parameters are chosen as they have been in this study.
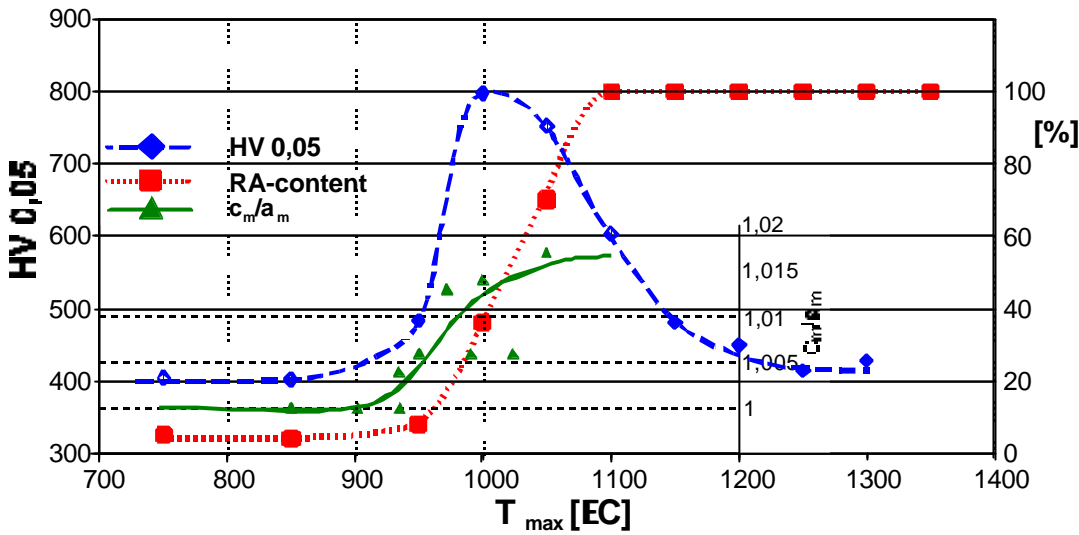

Figure 4: HV, c/a und RA vs. T_{max}

Fatigue Testing by 4-Point-Bending
Figure 5 presents the σ_a-N_f diagram of the 12 mm (T_{max}=1100°C, hardened zone, dashed line) and 16 mm (T_{max}=1100°C, hardened and tempered zones, dotted line) wide specimens in air in comparison to the base material (solid line). Obviously, the tensile residual stresses within the tempered zones have a detrimental effect on the fatigue properties. The number of cycles to failure (N_f) is about 6×10^4 for the base material at
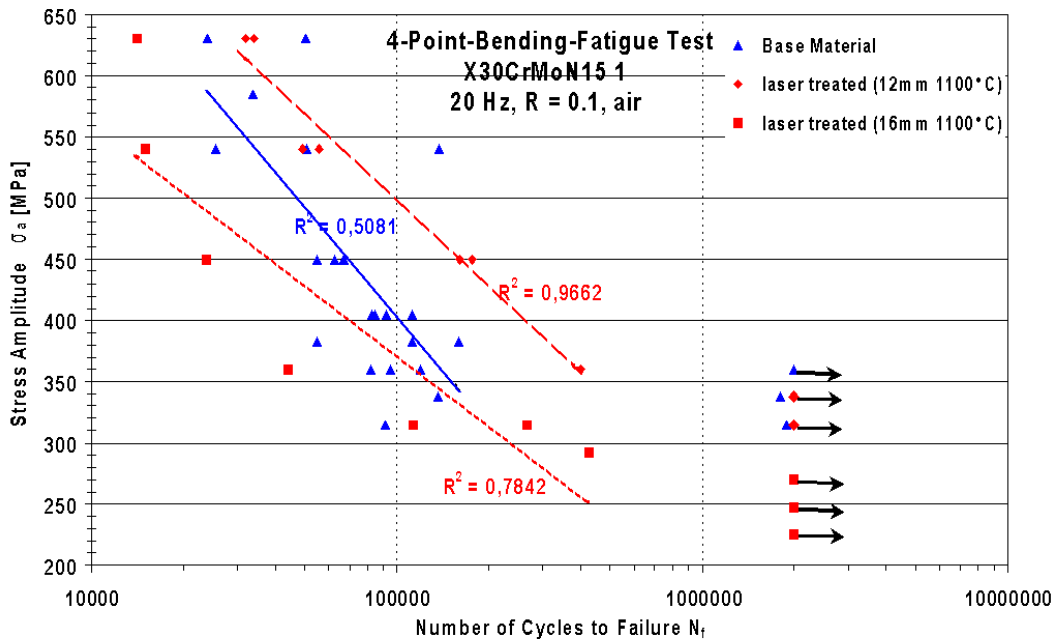

Figure 5: σ_a-N_f Diagram of 12 and 16 mm wide specimens

a stress amplitude of 450 MPa. The compressive residual stresses within the hardened zones bring about a N_f-value of $2x10^5$. This can be attributed to the fact, that the high compressive residual stresses distinctly decrease the effective stresses at the surface. Tensile residual stresses act in the opposite way and increase the effective stress. Thus, N_f drops down to a value of about $3x10^4$, which is a distinct loss of service life. The endurance limits of the base material and the hardened zones are similar and reach values of about 330 MPa, while the detrimental influence of the tempered zones brings about values below 270 MPa.

Artificial sea water seems to have a similar influence on fatigue as tensile residual stresses (T_{max}=1100°C, Figure 6). The trend lines of the narrow and the wide specimens are nearly equal and - within the accuracy available by the small number of data points - N_f ranges between 3 and $4x10^4$ for a stress amplitude of 450 MPa (dashed lines). The only measured endurance limit value is 270 MPa. Beside the fact that a higher number of tests will be necessary before one can draw a solid conclusion, it is obvious that the chemical attack by Cl-ions decreases the finite life as well as the endurance limit. This is true at least, if the surface consists of 100% RA supported by a hard subsurface martensitic layer, to which the compressive residual stresses are attributed. From potentiodynamic corrosion tests in aqueous 3%NaCl it is known, that the pitting potential just slightly differs between the base material and those laser heat treated at T_{max}=1100°C [5]. Thus, the chemical properties of the RA at the surfaces have no distinct influence on fatigue under corrosive environment. Other factors must, therefore, be more important.
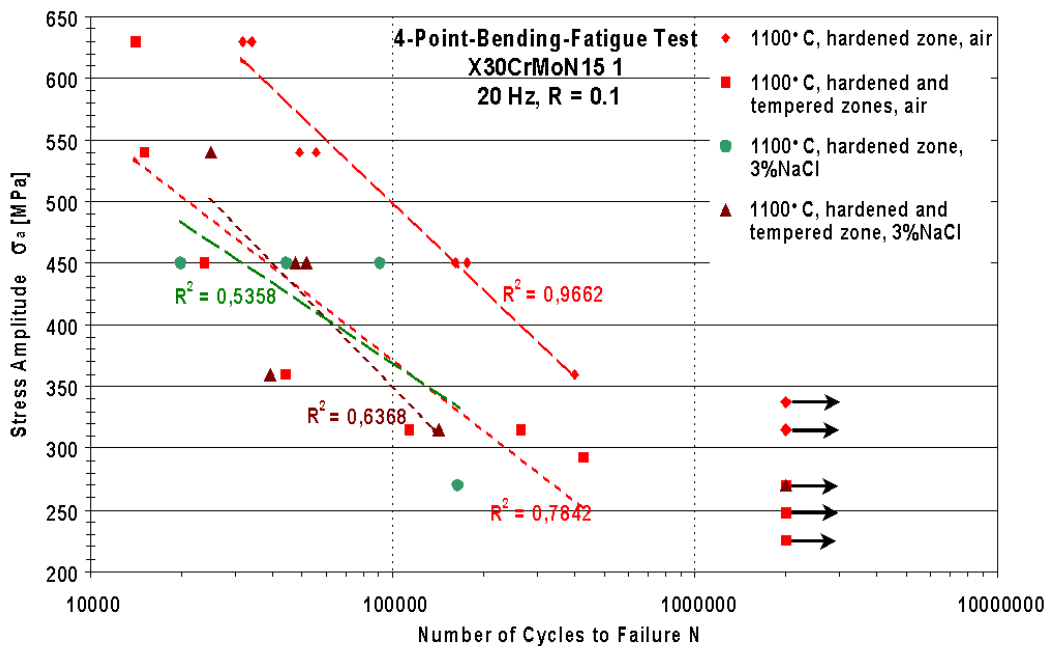

Figure 6: σ_a-N_f Diagram Comparison in Laboratory Air and 3%NaCl
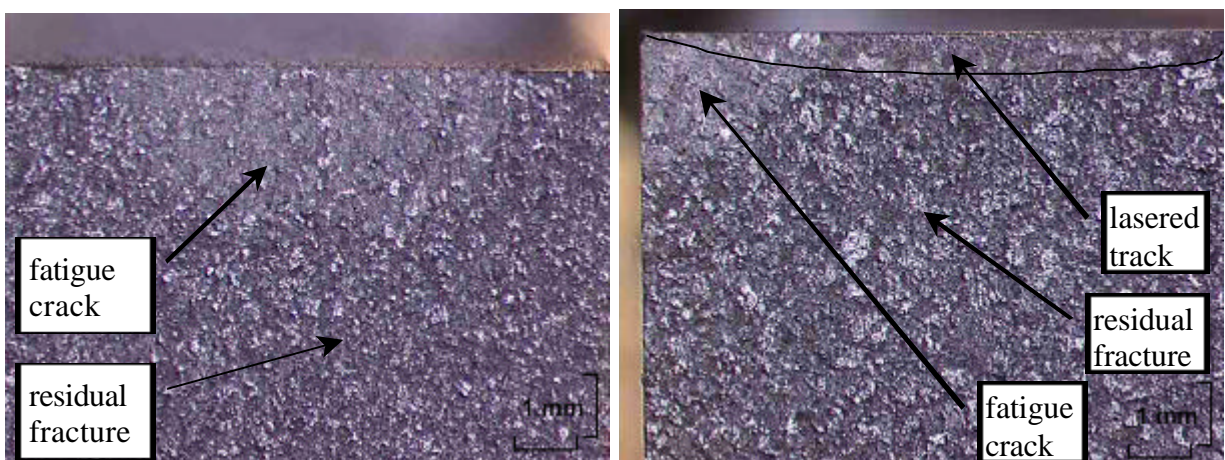

Figure 7: Fracture Surfaces with Edge and Half-Penny Shape Fatigue Cracks

Fractography renders, that crack initiations starts at or near the surfaces within the tempered zones (Figures 7a) or at the outer edge of the specimens (Figures 7b). The appearance of the fracture surfaces are typical for brittle fracture even though the fatigue crack area is somewhat smoother than the residual fracture. In

addition there is no difference between the appearances of the fatigue cracks generated in air compared to those generated under chemical attack. Nevertheless there is a difference in fatigue properties.

It is known from literature that martensitic tool steels often fail due to microstructural voids like coarse or eutectic hard phases, non-metallic inclusions, and pores, which act as internal local notches [7-10]. Due to the fact that the critical crack length a_c for unstable crack propagation is very small, it is concluded that the fatigue life of this type of tool steels is mainly governed by the number of cycles to crack initiation. If we examine those areas, where the fatigue cracks are likely to have started we find no signs of the common voids. But, there is some evidence that the former austenite grain boundaries act as notches (Figure 8). If we assume, that linear elastic fracture mechanics applies, ΔK_0 ranges from 3 to 5 MPa m$^{1/2}$ [7-11]. Now, a value of a_0 as a function of ΔK_0 and σ_a can be calculated, which is necessary to initiate stable fatigue crack growth [11, 12]. For an elliptical surface crack length a_0 might, therefore, range between 8 and 30 µm within the region of finite life. The compressive residual stresses should lower the values of σ_a and, thus, ΔK as well, bringing about higher critical crack length values. But, one has to keep in mind that the compressive residual stresses are only existing within the martensitic phase underneath the surface, while the austenite at the surface bares no or slight tensile residual stresses [13]. Due to the fact, that the former austenite grains have a size of about 100 µm they are likely to act as internal voids directly at and under the surface depending on the gradient of residual stresses and RA. Thus, crack initiation might take place at former austenite grains nearly independent of the measured residual stresses within the martensite, which might also relax during fatigue [14]. On the other hand it is known that the stress induced RA transformation brings about crack tip shielding effects [15]. This is most pronounced during crack propagation, which has a reported minor influence on fatigue life of martensitic tool steels.

But, this still does not explain the fact, that under 3%NaCl the numbers to failure are nearly independent of the residual stresses as shown in figure 6. The period of crack initiation must be similarly independent of the residual stress state at the surface. Otherwise, the measured values of N_f in 3%NaCl should differ distinctly between the 12 mm and the 16 mm wide specimens. This can only be attributed to the fact that ΔK_0 is lowered by corrosion as well. Thus, even smaller voids are critical and might act as cracks, which are able to propagate.

The influence of the competing mechanisms on crack initiation and propagation within the austenite is not clear, yet. There might be an early crack initiation, because of the tensile residual stresses within this phase. On the other hand the stress induced transformation of RA into martensite should distinctly slow down crack propagation. This has to be examined in detail in the future in order to be able to improve the fatigue life of parts and tools in air as well as under corrosive environment.
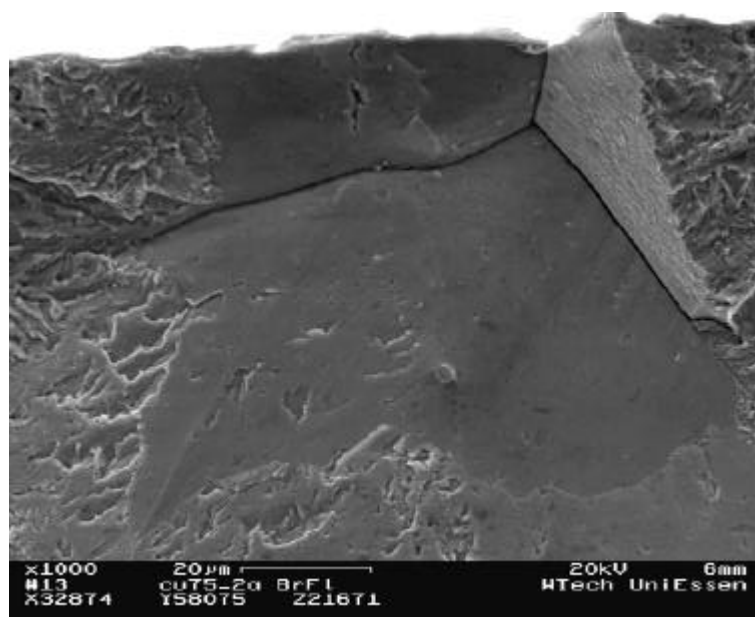

Figure 8: Crack Initiation at Former Austenite Grain Boundary

CONCLUSIONS AND OUTLOOK

An early crack initiation brought about by tensile residual stresses or stress corrosion cracking decreases finite fatigue life as well as the endurance limit.

Compressive residual stresses improve the fatigue behaviour in air, only.

More specimens are needed, because the coefficient of determination is often under 0.5.

Testing of specimens are necessary after grinding, because this changes the chemical, fatigue and wear properties due to the transformation of the RA bringing about additional compressive residual stresses within the surfaces.

ACKNOWLEDGEMENTS

REFERENCES

1. Berns, H., Lueg, J. (1990) *Neue Hütte* 36, 1, Pp.13-18.
2. Berns, H., Wang, G. (1993) in (Proc.Conf.) Bando, Y., Kosuge, K. (Eds.) Powder Metallurgy World Congress, Kyoto, Japan, Pp.513-516.
3. Berns, H., Escher, C., Streich, W.-D. (1998) *Ingenieur-Werkstoffe* 7, 3, Pp.36-39.
4. Bohne, C., Pyzalla, A., Reimers, W., Heitkemper, M., Fischer, A. (1998) in (Proc.Conf.) ECLAT ´98, Hannover, Germany, DGM-Informationsgesellschaft mbH, Frankfurt, Germany Pp.183-188
5. Pyzalla, A., Bohne, C., Heitkemper, M., Fischer, A. (2000) in (Proc.Conf.) Progress in Heat Treatment and Surface Engineering, E.J.Mittermeijer, J.Grosch (Eds.) 5th ASM Heat Treatment and Surface Engineering Conference, Gothenburg, Sweden. ASM, Metal Park, Ohio, USA, Pp.299-309
6. Heitkemper, M., Fischer, A., Bohne, C., Pyzalla, A. (2001) in (Proc.Conf.) Wear of Materials 2001, Vancouver, BC, Canada, D.Rigney et al. (Eds.) Elsevier, Amsterdam, The Netherlands, to be published
7. Berns, H., Trohjahn, W., Wicke, D. (1987) HTM 42, 4 Pp.211-216
8. Berns, H., Lueg, J., Trohjahn, W., Wähling, R., Wissell, H. (1987) Powder Met. Int. 19, 4 Pp.22-26
9. Berns, H. (1990) in (Proc.Conf.) 4th Int. Conf. on Fatigue 90, Honolulu, Hawaii, USA Eds. H. Kitagawa, T. Tanaka, Materials and Component Engineering Publications Ltd. Pp. 161 - 166
10. Melander, A. (1990) Int. J. of Fatigue 12, 3 Pp. 154-164
11. Schwalbe, K.H., (1980) Bruchmechanik metallischer Werkstoffe, Hauser, München, Wien Pp.646-654
12. Tada, H., Paris P.C., Irwin G.R., (1973) The Stress Analysis of Cracks Handbook, Del Research Corporation, St. Louis, MO, USA
13. Bohne, C., (2000) Mikrostruktur, Eigenspannungszustand und Korrosionsbeständigkeit des kurzzeitlaserwärmebehandelten hochstickstofflegierten Werkzeugstahls X30CrMoN15 1, Diss. TU Berlin, see also Berichte des HMI B572
14. Hauk, V., Nikolin, H.J. (1988) in (Proc.Conf.) ICRS 2, Nancy, France, 23.-25.11. 1988, Edited by G. Beck; S. Denis; A. Simon, Societe Francaise de Metallurgie, Elsevier Applied Science, Pp.895-900
15. Ritchie, R.O. (1987) in (Proc.Conf.) 5th Intern. Conf. on Mechanical Behavior of Materials, ICM 5, ASME, The Chinese Society of Metals, Beijing, China, Pp. 285-294